3D Finite Element Analysis of Curved Blade's Mechanics in Farming Tillage Operations

A. Armin*, W. Szyszkowski, R. Fotouhi,

***Abstract*—This paper is part of a study to develop robots for farming. As such power requirement is an important factor to operate equipment attach to such robots. Predicting accurately the forces which act on the blade during the farming is very important for optimal designing of farm equipment, as soil-tool interaction plays major role in power consumption, thus. In this manuscript a finite element (FE) investigation of soil–blade interaction is presented for curved-shape blades. The focus is on modeling and behavior of a blade with different rake angles and different curvatures that moves through a block of soil. The soil considered is an elastic-plastic material with non-associated Drucker-Prager constitutive law. In order to consider connection between soil surfaces, soil-blade and soil-soil surfaces, special use of contact elements are employed. A new separation criterion is discussed and a procedure to evaluate the forces acting on the blade is described in detail. The developed FE model and the procedures used the FE results are compared with analytical results available for straight blades from classical soil mechanics theories to verify correctness of the proposed FE model. Then the effects of blade's curvature and rake angle on blade force are examined. It is believed that the simulation method described may be applied to the soil-tool interactions analyses for complicated shapes of a blade and possibly for optimization of blades design.**

***Keywords*—Finite element analysis, soil-blade contact modeling, blade force, curve blade.**

I. INTRODUCTION

THE motivation of this study is to develop autonomous vehicles for agricultural setting to help farmers in crop production. Soil-tool interaction, especially tillage, is a procedure of preparing the soil for seeding. About half of energy used for crop production is consumed by tillage operation because of high draft force on tillage as [1] stated. This high energy consumption is not only because of the motion of large amount of soil mass, but also because of inefficient methods of energy transfer to the soil as [2] stated. All soil-tillage interaction researches have been focused to develop force prediction models by using different kinds of soil (soil physical and mechanical characteristics), tool (tool shape, tool's rake angle), and operating conditions (depth of cut, width of cut, travel speed, etc.) as [3] stated. Since blade shapes affect the shape and size of the soil failure one and consequently forces on the blade, optimization of the tillage-tool design will help to improve energy efficiency.

Due to the complex nature of the system, prediction of forces in analytical models is limited to simple rectangular blades shape. Therefore, analytical method cannot provide enough information for optimum design of a tillage-tool. Improvement in computers and computational techniques has led to the development of a new generation of highly efficient programs for simulating real situations with several parameters as [4] stated. Numerical techniques, especially finite element method (FEM), help to analyze the soil–tool interaction with the development of a suitable constitutive (stress-deformation) relation for specific working condition. FEM can be used to predict information about the failure zone, field of stress, soil deformation, acting forces on blades for agricultural equipment without limitation on the shape of blades. There are several models have been done based on finite element analysis (FEA), such as [5]-[8]. In these research works, they proposed different types of FE models to simulate soil-tool interaction and to obtain response of tools during these interactions.

From the numerical viewpoint soil separation is somewhat similar to the problem of cutting chips in machining operations [11]-[13], where various geometrical and physical separation criteria were developed based on critical values of displacements, strains, stresses, or strain energy to estimate the beginning of separation. A new criterion that uses the limit compacting strains in the direction of cutting is proposed here. When using this criterion to the FE model the soil particles are separated 'discretely' at consecutive nodes starting from the node that is nearest to the cutting edge of the blade.

The overall objective of this research work is to develop a simulation procedure for modeling the soil-tool interaction for arbitrary shape of the blade. Here the proposed procedure is tested on the straight blades in order to compare it with available analytical/experimental results [9], [10]. In particular, the use of contact elements, modeling sliding and cutting as the blade moves through the soil is explained in detail, as well as the method of calculating the draft force for the separation process that in fact takes place discretely at successive nodes. The soil selected for this study is the type of soil commonly found in Saskatchewan.

Ahad Armin is with Mechanical Department of Red Deer College, Canada (e-mail: ahad.armin@rdc.ab.ca).

Walerian Szyszkowski is with Mechanical Department of University of Saskatchewan, Canada (e-mail: walerian.szyszkowski@usask.ca).

Reza Fotouhi is with Mechanical Department of University of Saskatchewan, Canada (e-mail: reza.fotouhi@usask.ca).

ISBN: 978-988-14048-0-0
ISSN: 2078-0958 (Print); ISSN: 2078-0966 (Online)

II. Constitutive Law for Soil

In this research, the soil-blade interaction is modeled by the Drucker-Prager criteria with a non-associate flow rule controlled by the value of dilatancy angle v, which represents the volumetric expansion and frictional-dilatancy behavior of the material. If there is no volumetric expansion, then $v = 0$ (shear type of deformation only), which corresponds the direction 3 (vertical) of the increments of plastic strain in Fig. 1. On the other hand, for the flow rule associated with criterion (1) the increments of plastic strains would have direction 1 that contains shear deformation and dilatations characterized by the dilatancy angle $v = \varphi$. According to [14] for real materials angle v is usually less than φ and should be within the limits $0 < v < \varphi$ as indicated by direction 2 (the values of parameters used in the paper are listed in Table I).

In the numerical analysis with the external load increasing a typical material behavior defined by this law is plotted with dotted curve. It starts with elastic deformations until the yield criterion is reached and then the curve lines up with the yield surface (points are on this surface). Plastic deformations generated along the yield surface may be considered as compacting.

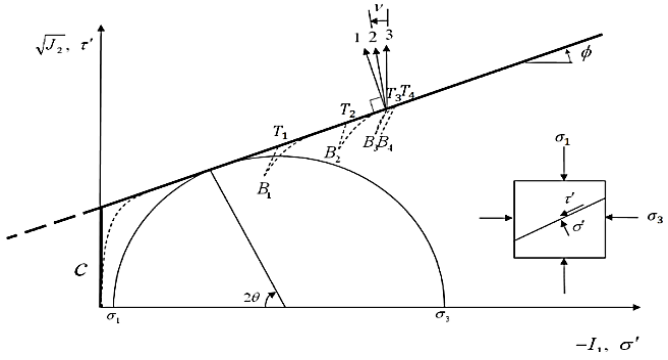

Fig. 1 The Drucker-Prager material law with non-associated flow rule

Since the separation status in FE can only be defined at nodes, the simulated separation process is 'discrete' in this sense that there would be some stress relieve when the status at a particular node is changed from initially connected to separated. For example if just before the first separation the stress state is defined by T_1 then just after separation it will be lowered and back in the elastic region. In this region the highest stress state, defined by B_1, will be typically at the opening's tip, i.e. at the node to be separated next. Then after a further load increase (controlled here by the forced blade's displacement) the stress state is observed at the node that would separate next. This stress state must first reach the yield surface again and then followed it until arriving at point T_2 where the separation criterion is met again. After separating at the subsequent node the stress state drops to B_2, and so on.

III. Material and Methods

A. FE Modeling

In the FE general 3D model both soil and blade are represented by the hexahedral elements SOLID45 from the ANSYS [15] library of elements, which have 8 nodes and 3 degree of freedoms (DOF) at each node. The soil-blade connection is modeled by the contact elements CONTACT173 and TARGET170 placed along the separation surfaces as discussed in the next section. Several meshing patterns were tried to verify convergence. Due to a large number of equilibrium iterations required for convergence, the calculations are generally long (typically lasting several hours on a computer with Intel core i5 4 GHz processor and 3.2 GB of RAM). Thus for computational efficiency and to make a balance between computational effort and accuracy, each model was meshed with higher density near the contact areas, and only the models that can be considered converged are shown in this study.

B. FE Model Description

Geometry of the FE model is sketched in Fig. 2. The model is parametric with several parameters defining the geometry of soil and tool. The soil block is $L_s = 300mm$ long, $w_s = 300mm$ wide, and $d_s = 150mm$ deep. These dimensions were selected in such a way that the solution in the vicinity of the blade is not sensitive to the block's size. The starting point of the blade's travel in the soil block is denoted by $L_e = 115mm$, and $L_f = 50mm$ is maximum distance blade can travel while cutting the soil (which is also length of contacts between upper and lower blocks of soil). These dimensions will be justified later. Parameter w_1 is the width of cut soil (also the width of blade), w_2 is the side width of soil block (note that $w_1 + 2w_2 = w_s$). The depth of blade inside the soil is d_1; which is also called the cutting depth of blade. The cutting portion of the blade is defined by three parameters $\alpha, \alpha_c,$ and d_1 where α is the angle of the blade's tip with respect to horizontal separation plane (the rake angle), and α_c is the angle of blade at the soil surface. The blade's total height is $h_1 = 100mm$, this parameter does not affect the cutting process. The other parameters shown in Fig.3, such as α_{avg}, the average blade slope, β, the blade's arc angle, and R, the blade's radius of curvature can be calculated from:

$$\alpha_{avg} = \frac{\alpha_c + \alpha}{2}, \quad \beta = \alpha_c - \alpha, \qquad R = \frac{d_1}{cos\alpha - cos\alpha_c} \tag{1a, 1b, 1c}$$

Table II lists values of the above parameters which were used in the first phase of the study. In the next phase, the effects of the angles α, and α_c on the force acting on the blade are examined (which through equations (6) can be interpreted as effects of the blade's curvature).

ISBN: 978-988-14048-0-0
ISSN: 2078-0958 (Print); ISSN: 2078-0966 (Online)

TABLE I
SOIL AND BLADE PARAMETERS USED IN PRESENT ANALYSIS

Properties	Soil	Blade
C- Cohesion	$20Kpa$	
φ- Soil internal friction angle	35°	
v - Dilatancy angle	20°	
$\bar{\omega}$- Soil water content	7%	
E - Modulus of elasticity	5 Mpa	200000 5 Mpa
μ - Poisson's ratio	0.36	0.3
ρ - Density	1220 $\frac{Kg}{m^3}$	7850$\frac{Kg}{m^3}$
φ_b - Blade-soil friction angle	23°	

TABLE II
SOIL-TOOL MODEL DIMENSIONS THAT USED IN FIRST MODEL ANALYSIS

$w_1(mm)$	$d_1(mm)$	$L_f(mm)$
50	50	50
$L_e(mm)$	$\alpha(^{\circ})$	$\alpha_c(^{\circ})$
115	60-75-90	35-45-60-75-90

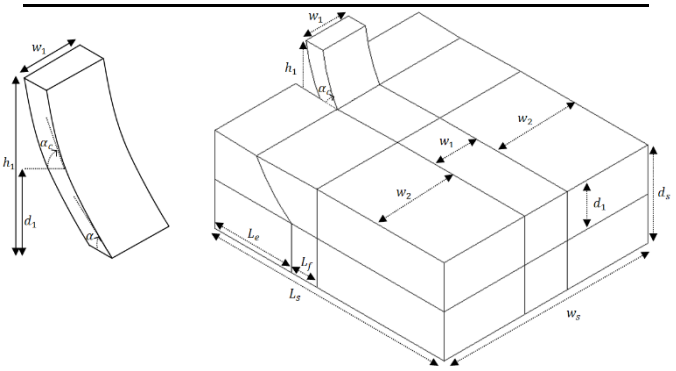

Fig. 2 3D soil-tool model and dimensions for narrow blade

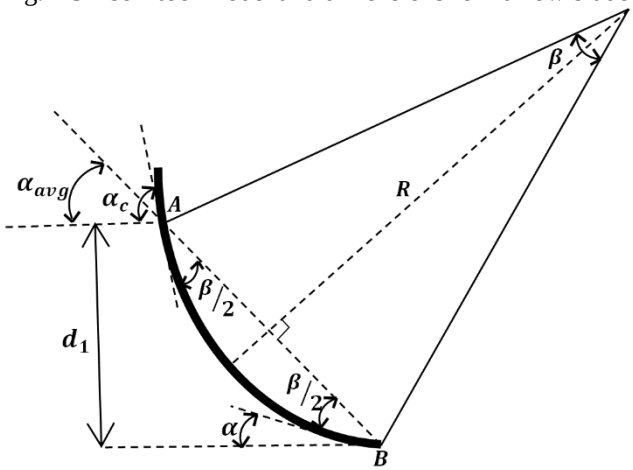

Fig. 3 Parameters characterizing a curved blade

C. Interaction Modeling

The soil-tool interaction is modeled using the ANSYS contact elements CONTACT173 and TARGET170 on four surfaces shown in Fig. 4. Contact elements with both bonding and sliding options are used to model soil separation (soil-soil) along three surfaces, 1 and 3 (for vertical cuts) and along the surface 2 (for horizontal cut). These surfaces will be referred to as the separation surfaces. However, on the surface 4 (referred to as the sliding surface), there is no soil separation and the soil is allowed to slide along surface of the blade (soil-blade contact), therefore the contact elements with only sliding option are used.

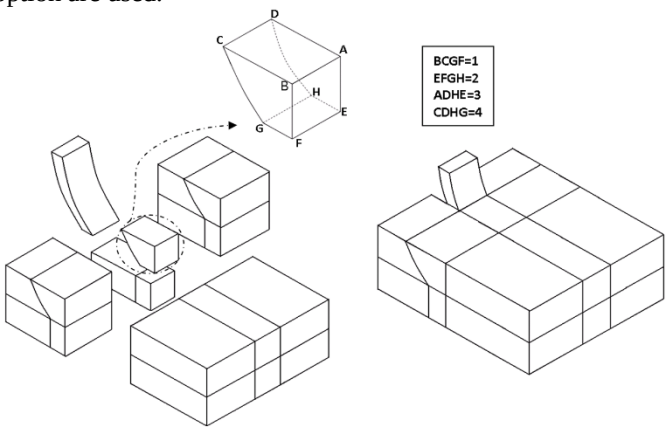

Fig. 4 3D Soil-blade model with contact surfaces. (1, 2, 3: contact surfaces with bonding and sliding option, 4: contact surface with sliding option)

The separation and sliding surfaces are actually two surfaces connected by the contact elements as indicated in Fig. 5 (this picture is not to scale). Any relative soil motion takes place on these surfaces during the soil-blade interaction. The separation surfaces are parallel to the direction of the blade's motion (only the line representing the horizontal separation surface is shown), while the sliding surface is parallel to the blade.

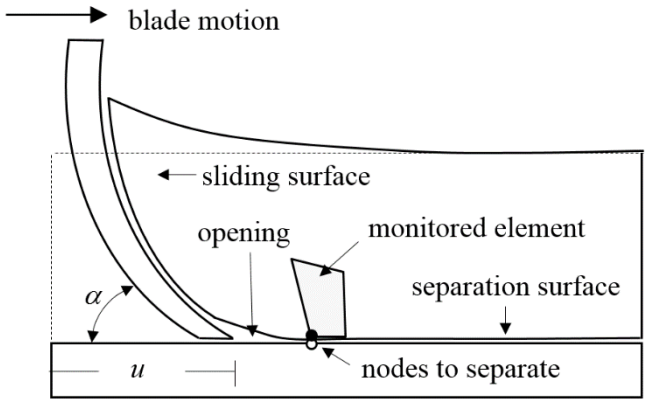

Fig. 5 Schematic details of modeling a blade-soil interaction

D. The Separation Principle

The elements above and below the expected separation surface are connected at nodes using the contact elements that

ISBN: 978-988-14048-0-0
ISSN: 2078-0958 (Print); ISSN: 2078-0966 (Online)

allow to activate or deactivate the bonding forces between them. The highest stress/deformation level is observed always in the element which is at the tip of the opening and is of a particular interest during the whole simulation. At the beginning all bonding forces are active and this element (to be referred to as the tip element) is adjacent to the tip of blade. As the blade starts to move, stresses go through the elastic phase (see the broken line in Fig. 1) until the solid line representing the yielding condition (1) is reached (where the Drucker-Prager plasticity rules are followed). In the tip element the strain component ε_x (in the direction of the blade's motion) is monitored continuously. The elasto-plastic process will continue until ε_x reaches a predefined magnitude of ε_c (which may be referred to as the limiting compacting strain) with the stress state reaching point T_1 in Fig. 1. At this instant the force bonding the nodes at the opening's tip (of the tip element) is deactivated, and the node separate generating the first opening of length equal to the size of the element's side. This is also associated with the stresses being relieved to the state denoted by point B_1, which will again be inside the elastic range (i.e. inside the surface defined by the yielding condition), and a drop in the value of ε_x below ε_c. With the blade moving forward the stress state will be increasing to reach the yielding condition again but at the new tip of opening that is now away from the blade's tip. The strain ε_x will become equal to ε_c at T_2 and the node separate at this tip increasing the opening's length by the size of that element and causing the stress (and strain) relieve indicated by point B_2, and so on. The separation criterion, calculating forces on the blade and numerical experimentation to set a predefined magnitude of ε_c are explained in details in [16].

Some details of the meshing and opening after three separations are shown in Fig. 6. One can note in the enlarged picture that the elements above the separation line have shrunk about 30% in the horizontal direction, which is the consequence of assuming $\varepsilon_c = 0.3$.

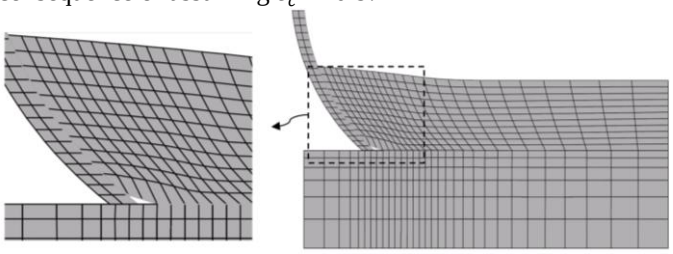

Fig. 6 The soil deformation after three separations (note the opening in front of the blade's tip)

IV. Results

A. Validation of The FE Model

As mentioned in Section 2, for straight rectangular blades the predictions of draft forces are available in [17]. In order to compare with these predictions, the straight blades($\alpha = \alpha_c$) with three different rake angles($\alpha = 60^\circ, 75^\circ, 90^\circ$) are analyzed. These three cases are modeled with the element size e = 8mm and compacting strain limit $\varepsilon_c = 0.3$. A typical plot of the blade forces calculated by the procedure presented in the previous section and the average forces plot $\overline{F}$ are shown in Figs.7 and 8. The average forces $\overline{F}$ are almost horizontal after the first iterations already, and the corresponding draft forces are $F_D = 605N, 540N$ and $440N$ for rake angles $\alpha = 90^\circ, 75^\circ$, and 60° respectively.

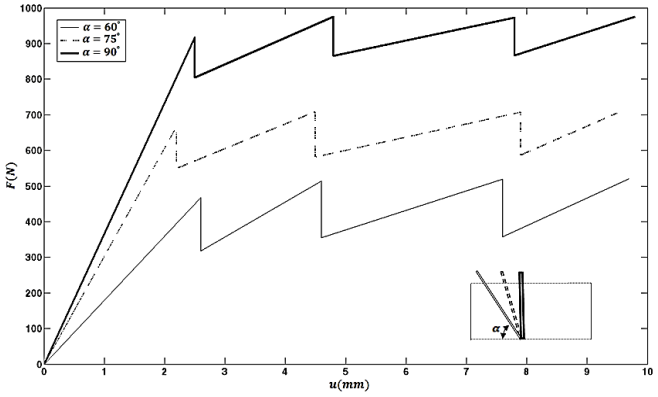

Fig. 7 Variation of draft forces for different rake angles and $\varepsilon_c = 0.3$

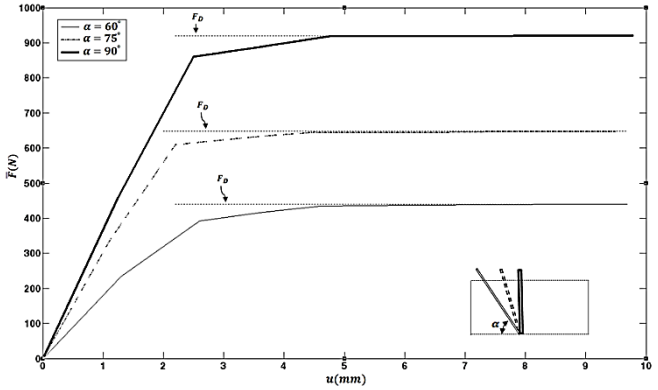

Fig. 8 Variation of the averaged draft forces for different rake angles and $\varepsilon_c = 0.3$

As can be observed the draft force acting on the blade becomes almost constant after the blade's motion of about 5mm inside the soil. It justifies the use of $L_f = 50mm$.

The following expression for the horizontal draft force was proposed in [17] for straight rectangular blades:

$$F_D^A = (\gamma_s d_1^2 N_{\gamma H} + c d_1 N_{cH} + Q d_1 N_{qH}) w_1 \quad (2)$$

Where γ_s is soil specific weight, c is soil cohesion, Q is bearing pressure (due to soil accumulation), d_1 is cutting depth of the blade inside soil and $(N_{\gamma H}, N_{cH}, N_{qH})$ are horizontal cutting factors that depend on the soil friction angle ϕ, and the blade rake angle α. In our case, for narrow blades $Q d_1 N_{qH} \approx 0$, while the factors $N_{\gamma H}, N_{cH}$ obtained from [10] are listed in Table III for different rake angles and constant ratios of the blade width (w_1) over the cutting depth (d_1).

ISBN: 978-988-14048-0-0
ISSN: 2078-0958 (Print); ISSN: 2078-0966 (Online)

TABLE III
THE CUTTING FACTORS FOR THE CASES PRESENTED IN FIG. 2.

Rake angle (α°)	$\boldsymbol{w_1/d_1}$	$N_{\gamma H}$	N_{cH}
90°	1	8.65	17.96
75°	1	7.15	13.56
60°	1	4.94	9.25

Using these factors and parameters from Table III in equation (2) the draft force on the blade are calculated and compared with FE results as shown in Table IV.

TABLE IV
COMPARISON BETWEEN FE AND ANALYTICAL RESULTS FOR DIFFERENT BLADE RAKE ANGLES

Rake angle (α°)	FE $F_D(N)$	Analytical F_D^A	Difference %
90°	1	8.65	17.96
75°	1	7.15	13.56
60°	1	4.94	9.25

As shown in Table IV, differences between these three models are relatively low which is another indication on validity of our method used in the FE simulation.

B. Effect of changing blade's curvature on draft force

Three FE models are studied in order to investigate the effects of changing the radius of curvature of the blade while keeping the rake angle constant. The shapes of curved blades are shown in Fig. 9 (a), (b), (c) and are controlled by the angle α_c that increases from 60° to 90°. For Fig. 9 (a), since $\alpha = \alpha_c = 60^{\circ}$ the blade is actually straight. From Fig. 10 it is obvious that by decreasing the radius (or increasing the curvature) while keeping the rake angle constant the blade force increases. It should be noted that also the blade's average rake angle α_{avg} is increasing from 60° to 75°. Fig. 11 depicts how this parameter affects the blade force that increases from 440N to 605N. In the other words this means more inclined blade requires less draft force to move inside the soil.

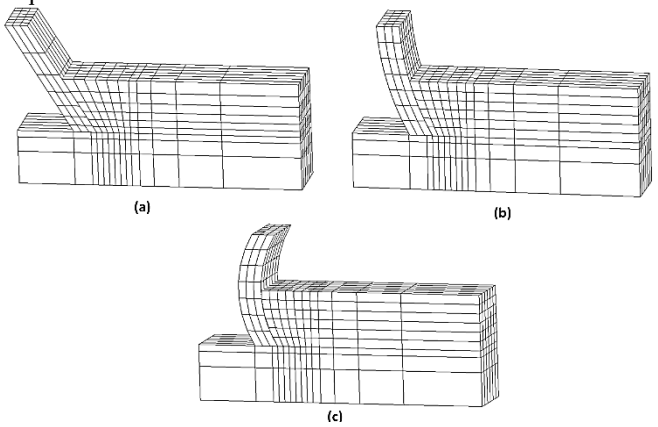

Fig. 9 FE models for $\alpha = 60^{\circ}$and different α_c, (a) $\alpha_c = 60^{\circ}$, (b) $\alpha_c = 75^{\circ}$, (c) $\alpha_c = 90^{\circ}$.

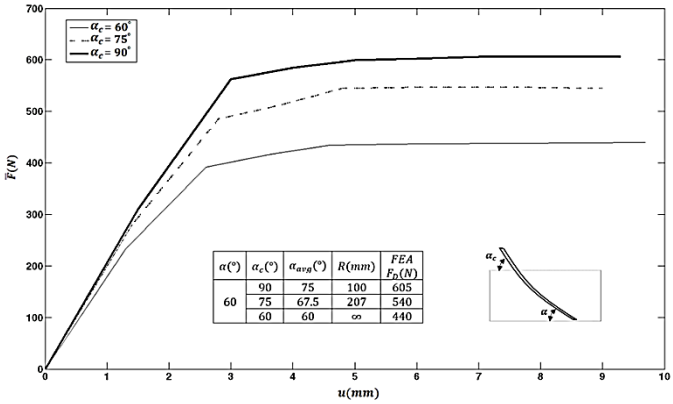

Fig. 10 The averaged draft forces for different α_c for the rake angle $\alpha = 60^{\circ}$.

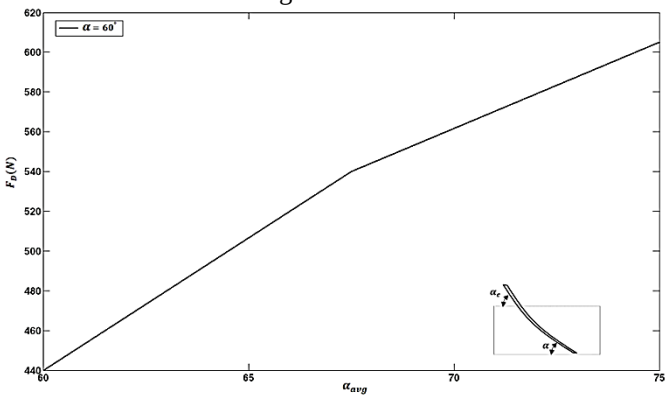

Fig. 11 The draft forces with different blade's average rake angles for $\alpha = 60^{\circ}$.

C. Some Deformation Results

Figures 12-13 show deformation of soils after the blade has been moved by about 7mm. As seen in Fig. 12 (a) and (b), in front of the blade the soil has swelled up in upward and lateral directions with respect to its original configuration in a pattern similar to that indicated in Shumulevic [18]. Also, each layer of soil above separation surface is pushed upward in a convex form as shown in Fig. 13.

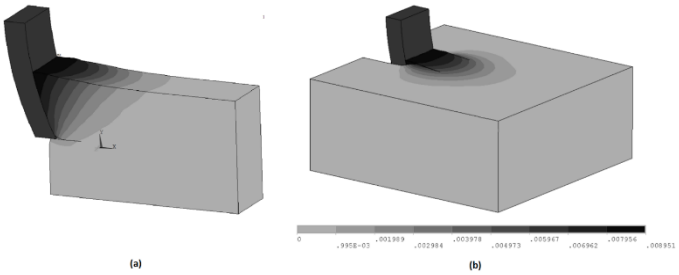

Fig. 12 Displacement patterns of the soil at u=7mm: (a) in front of the blade, (b) at the top surface.

ISBN: 978-988-14048-0-0
ISSN: 2078-0958 (Print); ISSN: 2078-0966 (Online)

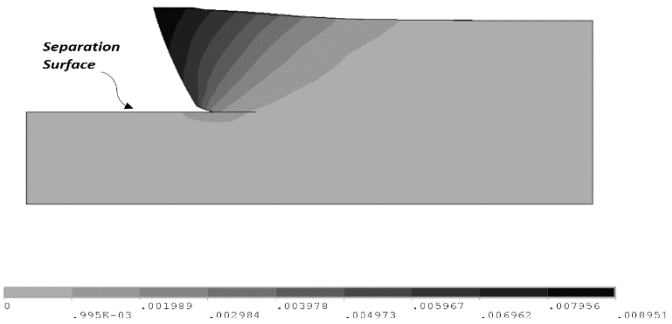

Fig. 13 Details of displacement of soil in front of the blade at u=7mm.

V. Conclusion

In this paper a new procedure for simulating the soil–blade interaction by the Finite Element Method is presented, which combines the Drucker-Prager non-associated constitutive law with a compaction strain based separation criterion to describe the behavior of soil while being cut by the blade. Several separation and sliding surfaces were defined and utilized in the analysis. The elements on these surfaces were bonded to each other using contact elements, however during motion of blade through soil, the bonding along the separation surfaces were allowed to break, resulting separation of the soil elements in front of the blade. The proposed model verified as simulation results from FEA had good correlation with analytical soil mechanics findings for straight blades. Also the effects of curved blade's geometrical parameters on the draft force were examined permitting to relate this force to the blades curvature, rake angle, etc. The procedure presented here can be extended to the analysis of blades of arbitrary shapes, which in turn can be used in optimization of the tillage operations.

References

[1] Zhang, J., and Kushwaha, R.L. 1998, "Dynamic analysis of tillage tool: Part I – Finite element method", Canadian Agriculture Engineering; Vol (40), pp. 287-292.

[2] Ashrafi Zadeh, S.R, 2006. "Modeling of energy requirements by a narrow tillage tool'. Unpublished Doctoral Thesis at the University of Saskatchewan, Saskatoon, Canada.

[3] S.Karmakar, 2008, "Modeling of soil-tool interaction in tillage". Transworld research network, India.

[4] M. Abo-Elnor, R. Hamilton, J.T. Boyle, 2004, "Simulation of soil-blade interaction for sandy soil using advanced 3D finite element analysis", Soil & Tillage Research. Vol(75), pp. 61-73.

[5] J. Wang, and D. Gee-Clough, 1991, "Deformation and failure in wet clay soil. Simulation of tine soil cutting". Proc IAMC Conference Beijing, China. Pp. 219-226.

[6] L. Chi, and R.L. Kushwaha, 1989, "Finite element analysis of force on a plane soil blade". Canadian Agriculture Engineering, Vol(31), pp. 135-140.

[7] J. Shen, and R. L. Kushwaha, 1998, "Soil-Machine Interactions-A Finite Element Perspective", Marcel Dekker Inc. Publishers,.

[8] S.K. Upadhyaya, U.A. Rosa, and D. Wulfsohn, 2002, "Application of the finite element method in agricultural soil mechanics", Advances in soil Dynamics, PP. 117-153.

[9] D.R.P. Hettiaratchi, A.R., Reece, The calculation of passive soil resistance. Computers and Geotechnique. 24 (1974) 280-310.

[10] E. McKyes, O.S. Ali, The cutting of soil by a narrow blade. Journal of Terramechanics. 14 (1977) 43-58.J. Shen, and R. L. Kushwaha, 1998, "Soil-Machine Interactions-A Finite Element Perspective", Marcel Dekker Inc. Publishers,.

[11] J. M. Huang, J. T. Black, An evaluation of chip separation criteria for the fem simulation of machining. J. Manufacturing science and Engineering. 118 (1996) 461-469.

[12] Ng. Eu-Gene, D.K. Aspinwall, Modeling of hard part machining. J. Material processing technology. 127 (2002) 222-229.

[13] A.P. Markopoulos, Finite element method in machining process. Springer, London, 2013.

[14] Y. Chen, L. J. Munkholm, T. A. Nyord, Discrete element model for soil-sweep interaction in three different soils. Soil & Tillage Research. 126 (2013) 34-41.

[15] Ansys version 11.0: Standard user's manual, 2008. Available from www.ansys.come

[16] A. Armin, R. Fotouhi, W. Szyszkowski, On the FE modeling of soil–blade interaction in tillage operations, Finite elements in analysis and design 92(2014)1-11.

[17] E. McKeyes, Soil cutting and tillage. Elsevier Science Publishing Company, New York, 1985.

[18] I. Shmulevich, Z. Asaf, D. Rubinstein, Interaction between soil and a wide cutting blade using the discrete element method. Soil & Tillage Research. 97 (2007) 37–50.

ISBN: 978-988-14048-0-0
ISSN: 2078-0958 (Print); ISSN: 2078-0966 (Online)